University of Pennsylvania
ScholarlyCommons

Departmental Papers (CBE)

Department of Chemical & Biomolecular Engineering

March 2007

The Stability of LSF-YSZ Electrodes Prepared by Infiltration

Wensheng Wang
University of Pennsylvania

Michael D. Gross
University of Pennsylvania

John M. Vohs
University of Pennsylvania, vohs@seas.upenn.edu

Raymond J. Gorte
University of Pennsylvania, gorte@seas.upenn.edu

Follow this and additional works at: http://repository.upenn.edu/cbe_papers

Recommended Citation

The Stability of LSF-YSZ Electrodes Prepared by Infiltration

Abstract

Composite electrodes were prepared by adding 40 wt % $La_{0.8}Sr_{0.2}FeO_3$ (LSF) into porous yttria-stabilized zirconia (YSZ) and their performance was studied as a function of time and calcination temperature. X-ray diffraction (XRD) patterns of the LSF-YSZ composites indicated an expanded lattice parameter after calcination above 1523 K, suggesting that Zr reacted with the LSF to form a Zr-doped perovskite; but XRD provided no evidence for reaction between LSF and YSZ after calcination at 1373 K or after operation for 1000 h at 973 K and 700 h at 1073 K. A composite of 40 wt % $La_{0.8}Sr_{0.2}Fe_{0.9}Zr_{0.1}O_3$ in YSZ showed reasonable performance at 973 K, with an area-specific resistance (ASR) of 0.22 Ω cm^2. Based on symmetric-cell measurements, electrodes calcined at 1123 K showed an initial ASR of 0.13 Ω cm^2 at 973 K but this increased linearly with time to 0.55 Ω cm^2 after 2500 h at 973 K. However, the ASR depended strongly on current density, decreasing dramatically under both anodic and cathodic polarization. Electrodes calcined at 1373 K showed an ASR of 2.5 Ω cm2 at 973 K but this value also decreased dramatically under polarization. Scanning electron microcopy images demonstrate that aging at 973 K and calcination at 1373 K cause significant sintering of the LSF. It is therefore suggested that deactivation is caused by morphological changes, rather than solid-state reactions, with a dense layer of LSF forming over the YSZ substrate.

Keywords

lanthanum compounds, strontium compounds, yttrium compounds, zirconium compounds, electrodes, composite materials, calcination, lattice constants, electrical resistivity, anodisation, scanning electron microscopy, ageing, current density, sintering, melt infiltration, porous materials, ceramics

Comments

The Stability of LSF-YSZ Electrodes Prepared by Infiltration

Wensheng Wang,* Michael D. Gross, John M. Vohs,* and Raymond J. Gorte*,z

Department of Chemical and Biomolecular Engineering, University of Pennsylvania, Philadelphia, Pennsylvania 19104, USA

Composite electrodes were prepared by adding 40 wt % $La_{0.8}Sr_{0.2}FeO_3$ (LSF) into porous yttria-stabilized zirconia (YSZ) and their performance was studied as a function of time and calcination temperature. X-ray diffraction (XRD) patterns of the LSF-YSZ composites indicated an expanded lattice parameter after calcination above 1523 K, suggesting that Zr reacted with the LSF to form a Zr-doped perovskite; but XRD provided no evidence for reaction between LSF and YSZ after calcination at 1373 K or after operation for 1000 h at 973 K and 700 h at 1073 K. A composite of 40 wt % $La_{0.8}Sr_{0.2}Fe_{0.9}Zr_{0.1}O_3$ in YSZ showed reasonable performance at 973 K, with an area-specific resistance (ASR) of 0.22 Ω cm². Based on symmetric-cell measurements, electrodes calcined at 1123 K showed an initial ASR of 0.13 Ω cm² at 973 K but this increased linearly with time to 0.55 Ω cm² after 2500 h at 973 K. However, the ASR depended strongly on current density, decreasing dramatically under both anodic and cathodic polarization. Electrodes calcined at 1373 K showed an ASR of 2.5 Ω cm² at 973 K but this value also decreased dramatically under polarization. Scanning electron microcopy images demonstrate that aging at 973 K and calcination at 1373 K cause significant sintering of the LSF. It is therefore suggested that deactivation is caused by morphological changes, rather than solid-state reactions, with a dense layer of LSF forming over the YSZ substrate.

© 2007 The Electrochemical Society. [DOI: 10.1149/1.2709510] All rights reserved.

The standard material for cathodes in solid oxide fuel cells (SOFCs) is a composite of yttria-doped zirconia (YSZ) and Sr-doped LaMnO₃ (LSM),[1] despite the fact that the electrochemical performance of this material is only modest at intermediate temperatures and that significantly improved performance can be achieved by substituting the LSM with Sr-doped LaCoO₃ (LSCo)[2-5] or LaFeO₃ (LSF).[6-12] The primary reason for using LSM-based cathodes is that LSM-YSZ electrodes are relatively easy to fabricate and have excellent, long-term stability. LSM-YSZ electrodes can be prepared by simply sintering the mixed powders together on YSZ electrolytes, because formation of insulating layers of $La_2Zr_2O_7$ and $SrZrO_3$ occurs only at very high temperatures.[1,13] By contrast, LSCo undergoes solid-state reactions with YSZ, even at 973 K,[14] making it necessary to introduce an interlayer between LSCo and YSZ to avoid contact.

Whether LSM could be replaced by LSF is less clear, and a review of the literature leaves many questions unanswered about the stability of cathodes based on this material. Outstanding performance has been achieved with LSF-based cathodes[8,9,11] and a number of papers have reported stable operation for periods of at least several hundred hours using this material.[15] Furthermore, X-ray diffraction (XRD) measurements of cosintered mixtures of LSF and YSZ showed that new phases were not produced for temperatures up to 1673 K.[15] However, most studies of LSF electrodes have used doped-ceria interlayers to separate LSF from YSZ,[8,9] and some studies have incorporated CuO_x into LSF to allow the use of lower sintering temperatures.[16] Presumably, these steps are taken to avoid interfacial reactions between LSF and YSZ. Possible evidence for an interfacial reaction is the observation that annealing LSF-YSZ mixtures to 1473 K causes an expansion of the perovskite lattice, suggesting that the perovskite phase becomes Zr-doped at higher temperatures.[10] Given that the lattice expansion seems to be minimal after heating to 1273 K and that Zr-doped LSF may be conductive, one must conclude that questions still exist about why interlayers are required for LSF-based cathodes and whether LSF-YSZ composites could be stabilized.

At least some of the deactivation in previous work was associated with fabrication steps, because high-temperature annealing is usually required to sinter the cathode onto the electrolyte. To determine whether LSF-YSZ cathodes are intrinsically stable at SOFC operating conditions, we set out to investigate electrodes prepared by low-temperature methods. In our laboratory, we have demonstrated that we can prepare LSF-YSZ electrodes by impregnation of a porous YSZ matrix with La, Sr, and Fe salts, followed by relatively low-temperature reaction to form the LSF perovskite.[11] Because the porous YSZ is heated with the YSZ electrolyte to high temperatures prior to adding LSF, the initial performance of these composite cathodes is very good.

In this paper, we report a study of the stability of LSF-YSZ cathodes prepared by impregnation. The performance of these cathodes was measured as a function of time and annealing temperature. We show that the performance at 973 K of LSF-YSZ electrodes is unstable if they were initially calcined to only 1123 K. The characteristics of an LSF-YSZ composite electrode calcined to 1373 K were similar to those of the 1123 K composite after long-time operation at 973 K. While there was no evidence for solid-state reaction between LSF and YSZ at either 1373 K or at SOFC operating temperatures, the LSF phase was found to sinter significantly following high-temperature treatment or after long times operating at 973 K. Based on the data, we conclude that the LSF forms a dense coating on the YSZ pores and that transport of oxygen through the dense film limits the performance. Possible methods for stabilizing the impregnated composites are discussed.

Experimental

The initial experiments were performed on cells that were essentially symmetrical, with two LSF-YSZ electrodes separated by a 50 μm thick YSZ electrolyte, except that one of the LSF-YSZ electrodes was 50 μm thick and the other 300 μm thick to provide mechanical support. The first step in preparing the symmetric cells involved fabricating a YSZ wafer that had a dense layer, surrounded by 50 μm and 300 μm porous layers. This porous-dense-porous structure was produced by laminating three green tapes, using pore formers in the layers that were to be porous, and then firing the structure to 1823 K for 4 h.[17] The green tapes were prepared by mixing YSZ powder (Tosoh Corp., 8 mol % Y_2O_3-doped ZrO_2, 0.2 μm) with distilled water, a dispersant (1.27 g, Duramax 3005, Rohm & Haas), and binders (10.2 g HA12 and 14.4 g B1000, Rohm & Haas). To produce the 50 μm porous layer, graphite (GE, Alfa Aeser, 325 mesh, conductivity grade) was added to the mixture, while porosity in the 300 μm layer was obtained using a mixture of graphite and polystyrene pore formers.[11,18] The porosity of both layers was ~65%.

To produce LSF-YSZ composites, the porous YSZ was infiltrated with aqueous solutions of $La(NO_3)_3 \cdot 6H_2O$, $Sr(NO_3)_2$, and $Fe(NO_3)_3 \cdot 9H_2O$, at a molar ratio of La:Sr:Fe = 0.8:0.2:1. The so-

lutions also contained citric acid, with the concentration of citrate ions equal to that of the metal ions.[11,18] Each impregnation step was followed by calcination to 1123 K, and multiple impregnation steps were used to reach a final loading of 40 wt % LSF. An electrode made from Zr-doped LSF was synthesized in the same way, except that $ZrO(NO_3)_2 \cdot 6H_2O$, was included in the solution so as to achieve a final perovskite composition of $La_{0.8}Sr_{0.2}Fe_{0.9}Zr_{0.1}O_3$. After the electrodes were prepared, some were calcined to higher temperatures to determine how this affected the composite structure and performance.

The performance of the LSF-YSZ composites under fuel cell and electrolysis conditions was measured using cells with 300 μm, LSF-YSZ air electrodes and a 50 μm YSZ electrolytes. The fuel electrodes in these studies were prepared by impregnating porous YSZ layers, 12 μm in thickness, with 40 wt % ceria and 1 wt % Pd, and then applying Ag paste onto the external surface, as described elsewhere.[19] The cells were attached to an alumina tube with a ceramic adhesive (Aremco, Ceramabond 552). The external area of the fuel electrode was 0.33 cm^2 but the area of the electrolyte and air electrode were ~1 cm^2. While all of the results reported in this paper assume an active cell area of 0.33 cm^2, calculations using our cell parameters suggest that this may underestimate the active area by as much as 9%.[20] The fuel side in these studies was exposed to humidified H$_2$ (either 3 or 10% H$_2$O).

Impedance spectra were measured on both the symmetric cells and the fuel cells at various current densities in the galvanostatic mode, with a frequency range from 0.1 Hz to 100 KHz and a 5 mV ac perturbation, using a Gamry Instruments potentiostat. In all cases, Ag paste was used as the current collector under both air and fuel conditions. The spectra for the symmetric cells had an additional 0.2 Ω cm^2, ohmic contribution due to the lead wires, but, in the fuel-cell/electrolysis measurements, this contribution was removed through the use of reference leads. For the symmetric cells, the impedance data were multiplied by 0.5 to account for the fact that there are two electrodes contributing to the impedance.

The physical characteristics of the LSF-YSZ composite were examined by XRD and scanning electron microscopy (SEM). The XRD measurements were performed using Cu Kα radiation on samples which had KCl added to serve as an internal reference for the diffraction peak positions.

Results

Figure 1 shows XRD results for a 40 wt % LSF impregnated LSF-YSZ composite after calcination to various temperatures. Because the XRD data did not show phases other than that of YSZ and the perovskite, in agreement with results from previous studies,[10,11] the diffraction patterns are shown only in the region between 29.8° and 32.8° 2θ to focus on the YSZ (111) and LSF (orthorhombic 020/112) peaks. For calcination at 1123 K (Fig. 1a) the perovskite peak is broad, indicating small crystallites, but centered at the correct position for LSF, 32.28° 2θ. After testing this electrode for 1000 h at 973 K and an additional 700 h at 1073 K, the diffraction pattern of the composite changed to that shown in Fig. 1b. The peak associated with LSF has narrowed and shifted to slightly larger angles (32.34°), consistent with sintering of the LSF into larger crystallites. The diffraction pattern obtained from an LSF-YSZ composite that was heated for 1 h to 1373 K (Fig. 1c) is almost indistinguishable from that in Fig. 1b.

However, the pattern in Fig. 1d shows that heating the composite to 1523 K for 1 h causes a significant shift in the peak position for the LSF phase, to 32.15° 2θ. This expansion of the LSF lattice was observed in a previous study, where it was suggested that the change in lattice parameter is due to reaction with the YSZ to form a Zr-doped LSF.[10] In agreement with this assignment, a composite made by impregnating $La_{0.8}Sr_{0.2}Fe_{0.9}Zr_{0.1}O_3$ into porous YSZ (Fig. 1e) showed a very similar peak position for the LSF phase after calcination to only 1523 K.

To determine whether Zr doping could cause deactivation of
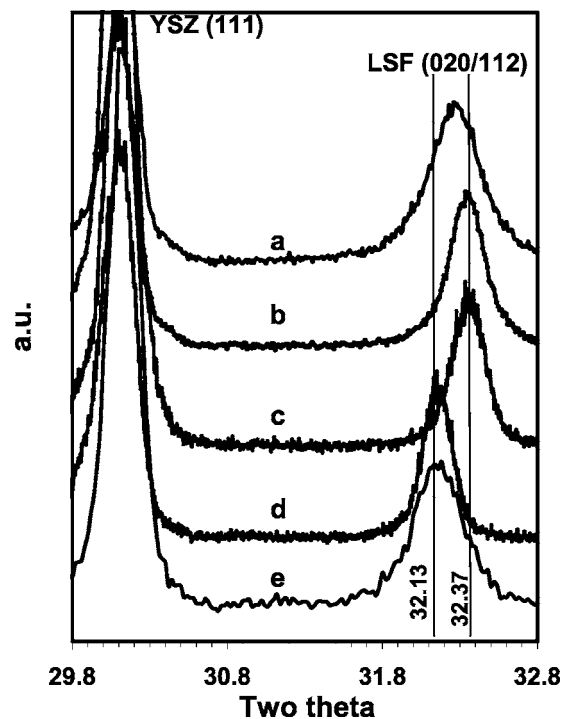
Figure 1. XRD data for LSF-YSZ composites following various pretreatments. Only the region between 29.8° and 32.8° 2θ is shown because no additional phases were formed. (a) Fresh LSF-YSZ calcined at 1123 K, (b) LSF-YSZ calcined at 1123 K, after exposure to air at 973 K for 1000 h and 1073 K for 700 h, (c) LSF-YSZ calcined at 1373 K, (d) LSF-YSZ calcined at 1523 K, and (e) $La_{0.8}Sr_{0.2}Fe_{0.9}Zr_{0.1}O_3$ calcined at 1123 K.

LSF, we tested otherwise identical symmetric cells made by impregnating 40 wt % LSF or $La_{0.8}Sr_{0.2}Fe_{0.9}Zr_{0.1}O_3$ into porous YSZ at 973 K. Because of slight differences (<0.05 Ω cm^2) in the ohmic resistances of the two cells, the ohmic contribution to the impedance data in Fig. 2 have been removed. The performance of the electrodes made from $La_{0.8}Sr_{0.2}Fe_{0.9}Zr_{0.1}O_3$ was worse than that for electrodes made from LSF, with an electrode impedance of 0.22 Ω cm^2 compared to 0.13 Ω cm^2 for the LSF electrode. However, the performance of the $La_{0.8}Sr_{0.2}Fe_{0.9}Zr_{0.1}O_3$-YSZ electrodes is still quite respectable, especially considering that the Zr-dopant level in the $La_{0.8}Sr_{0.2}Fe_{0.9}Zr_{0.1}O_3$-YSZ electrode is high compared to any possible doping that occurs with calcination at 1373 K or aging at 973 and 1073 K.

The effect of electrode aging for LSF-YSZ electrodes at 973 K, using a symmetric cell, is shown in Fig. 3. This plot reports both the
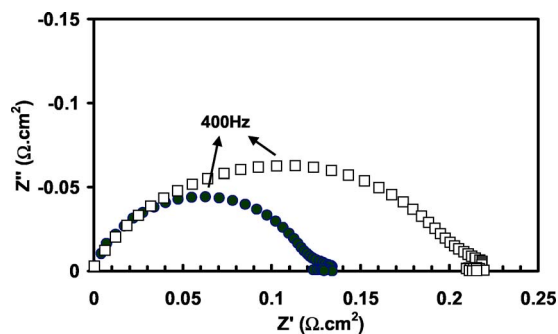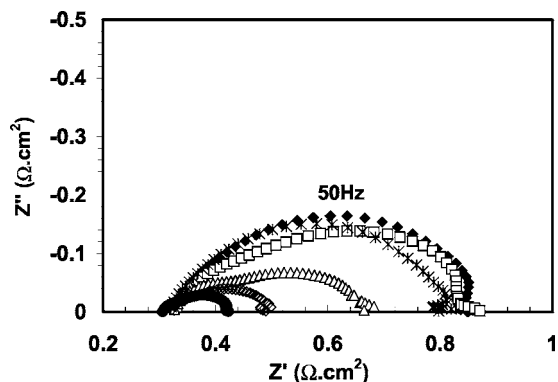

Figure 2. Impedance spectra measured on symmetric cells at 973 K of composites with 40 wt % perovskite in YSZ. The data are for LSF-YSZ (●) and $La_{0.8}Sr_{0.2}Fe_{0.9}Zr_{0.1}O_3$ (□) calcined at 1123 K.
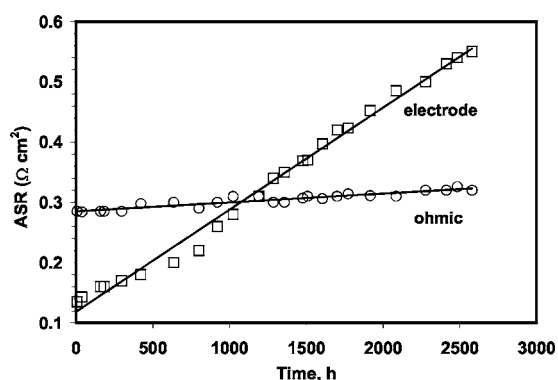
Figure 3. Impedance results for a symmetric cell at 973 K as a function of time for the LSF-YSZ electrodes calcined at 1123 K. Both the ohmic and electrode polarization impedances are shown.
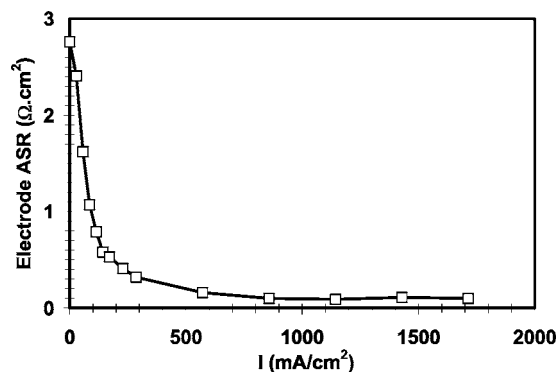

Figure 5. Cole-Cole plots for a symmetric cell with LSF-YSZ electrodes, calcined at 1373 K, tested at 973 K. The data are reported as a function of the current density applied to the cell: (♦) OCV, (□) 100 mA/cm^2, (△) 200 mA/cm^2, (◇) 400 mA/cm^2, and (●) 600 mA/cm^2.

ohmic contribution and the electrode polarization losses as a function of time for a period of more than 2500 h. The ohmic losses did not change appreciably over this period of time, and the total value of the ohmic resistance (when not multiplied by 0.5) agreed well with that expected for a 50 μm YSZ electrolyte (~0.3 Ω cm^2) and the lead wires (~0.2 Ω cm^2). However, the polarization losses grew substantially over time, from 0.13 to 0.55 Ω cm^2.

Because earlier measurements in our laboratory of symmetric cells with LSM-YSZ electrodes showed high polarization losses prior to activation by polarization,[18,21,22] we decided to examine the "deactivated" LSF-YSZ electrodes after passing a current through the cell. The results, shown in Fig. 4, were surprising and different from what was observed with LSM. First, unlike LSM, the LSF-YSZ electrodes did not exhibit hysteretic behavior. The impedance spectrum at open circuit, taken immediately after passing current through the cell, was essentially identical to the spectrum taken prior to polarizing the cell. Second, impedance spectra measured with an imposed current showed a dramatic decrease in the electrode impedances. Indeed, the symmetric-cell spectrum collected at a current density of 600 mA/cm^2 was similar to the spectrum obtained before electrode aging, with an electrode impedance of less than 0.13 Ω cm^2. In the presence of an applied current, the cell was no longer symmetrical and the measured impedance is the average of the two electrodes, one of which was polarized cathodically and the other anodically. Because the average electrode impedance decreased by more than a factor of two, this decrease must be occurring under both anodic and cathodic polarization. This is again very
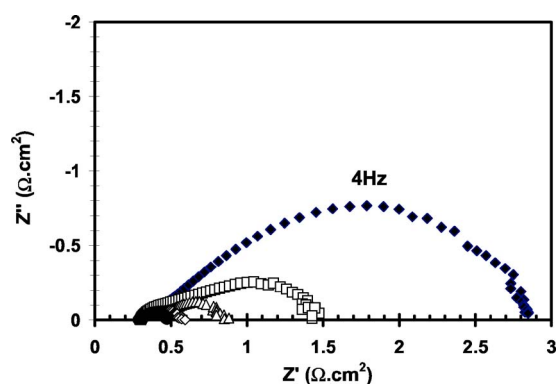
different from what was observed with LSM-YSZ electrodes, where only cathodic polarization decreased the impedance.[18]

The effect of electrode aging appears to be similar to the effect of increased calcination temperature. Figure 5 shows impedance spectra at 973 K for a symmetric cell with LSF-YSZ electrodes that were initially calcined to 1373 K, a temperature which is still sufficiently low so as to avoid a change in the lattice parameter of the perovskite phase, as shown in Fig. 1. Again, the ohmic resistance agrees well with the value expected for the electrolyte and lead wires; however, the electrode polarization losses at open circuit were very large, ~2.5 Ω cm^2. As with the cell held at 973 K for 2500 h, the impedance spectrum of this cell changed when a current was applied. For a current density of 600 mA/cm^2, the average electrode impedance decreased to less than 0.2 Ω cm^2. Again, the electrode showed no hysteretic behavior. Figure 6 provides a plot of the average electrode impedance as a function of the applied current density for the symmetric cell calcined to 1373 K. The impedance appears to drop almost exponentially with current density, although plots of either the electrode impedance or the cell potential vs the logarithm of the current density were not linear.

Additional proof that there is a similar origin for the effect of high-temperature calcination and 2500 h aging at 973 K on electrode impedance is provided by a stability test of the 1373 K symmetric cell. No changes were observed during a 700 h test of this cell at 973 K, suggesting that whatever processes were responsible for changing performance during the 2500 h, 973 K test in Fig. 3 simply occurred more quickly at 1373 K, resulting in the same final state.

Figure 4. Cole-Cole plots for the same symmetric cell used for the measurements in Fig. 3, tested at 973 K after 2483 h. The data are reported as a function of the current density applied to the cell: (♦) OCV, (□) 100 mA/cm^2, (△) 200 mA/cm^2, (◇) 400 mA/cm^2, (●) 600 mA/cm^2, and (*) OCV immediately after applying 600 mA/cm^2.

Figure 6. A plot of the average electrode polarization impedance of the symmetric cell with LSF-YSZ electrodes calcined to 1373 K as a function of current density.
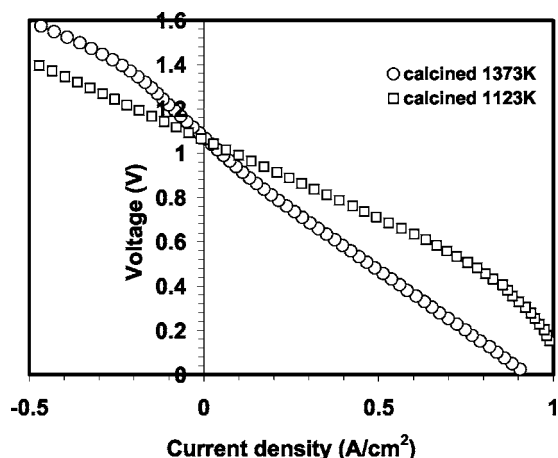
Figure 7. V-i polarization curves measured at 973 K for two cells with LSF-YSZ electrodes. The two cells were essentially identical, except that the electrode in one was calcined to 1123 K and the other to 1373 K.

Because the LSF-YSZ electrodes are affected by both anodic and cathodic polarization, the impedance spectra are complicated by convolution of these two effects in the presence of an applied current when using symmetric cells. Therefore, we examined cells that had one LSF-YSZ electrode under more normal fuel cell/electrolysis conditions. The air electrodes in these cells were identical to the thicker of the LSF-YSZ electrodes in the symmetric cells, having been made by impregnating 40 wt % LSF into porous YSZ, 300 μm thick. The LSF in one of the cells was calcined to 1123 K and the other to 1373 K. The electrolytes were 50 μm thick and the fuel electrodes are described above. The performance curves at 973 K holding the fuel electrode in a 10% H_2O-90% H_2 mixture for these two cells are shown in Fig. 7. Total-cell impedance spectra, taken at selected current densities, are shown in Fig. 8a and b.

The 1123 K cell shows a nearly linear V-i curve from −500 to 500 mA/cm^2 at 973 K, a result confirmed by the impedance data in Fig. 8a. The curvature in the V-i curve above 500 mA/cm^2 is associated with the fuel electrode and may be caused by diffusion of the fuel through the layer of Ag paste. The impedance spectra indicate that the total ASR of the cell is less than 0.7 Ω cm^2 for current densities from −500 to 500 mA/cm^2, in good agreement with the slope of the V-i curve. The electrolyte contribution to the total ASR is calculated to be ∼0.3 Ω cm^2, and there is an additional small contribution to the ohmic losses from the functional layer of the fuel electrode.[19] The 10 μm, Pd-doped, ceria-YSZ functional layer contributes approximately 0.1 to 0.2 Ω cm^2 to the nonohmic losses and an additional 0.1 Ω cm^2 to the ohmic losses which, as shown by the data in Fig. 8a, depend on the magnitude and sign of the current density. Based on these estimates of the fuel-electrode performance, the LSF-YSZ electrode exhibits an impedance between 0.1 and 0.15 Ω cm^2 that is independent of current density. This agrees with the losses measured using symmetric cells as shown in Fig. 2.

The data in Fig. 7 also shows that the cell made with the LSF-YSZ electrode calcined to 1373 K exhibited distinctly lower performance at 973 K. Furthermore, there is curvature in the V-i plot on both sides of open circuit, which is consistent with the impedance spectra in Fig. 8b. This cell showed a higher ohmic resistance, ∼0.5 Ω cm^2, probably due to variations in the cell fabrication. More important, the nonohmic impedance near open circuit was very large, almost 1.0 Ω cm^2; and this decreased dramatically under anodic polarization to 0.3 Ω cm^2 at −450 mA/cm^2. The decrease in the impedance was somewhat less dramatic under cathodic polarization, ∼0.5 at 450 mA/cm^2; but there may be an increase in the impedance of the fuel electrode at high current densities that counteracts the decrease in the air electrode.
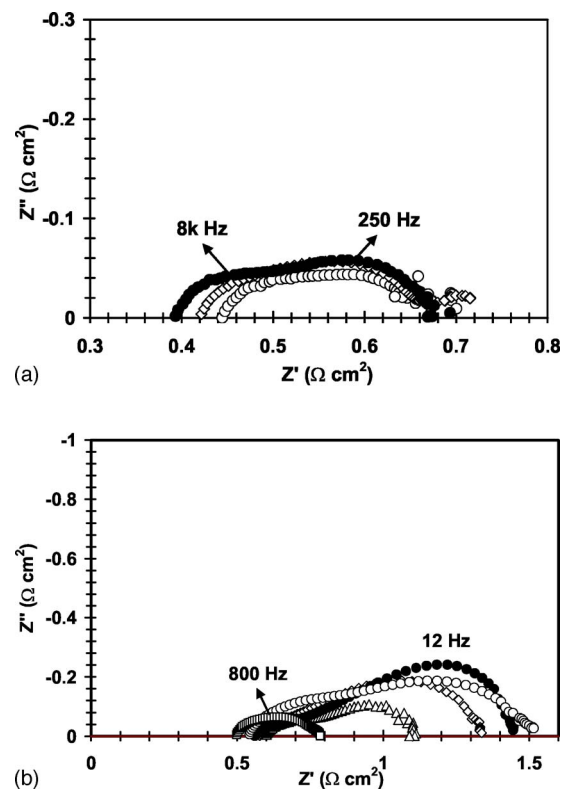

Figure 8. Cole-Cole plots at various current densities for the same two cells in Fig. 7. (a) Results for the cell with and LSF-YSZ cathode calcined to 1123 K: (○) 450 mA/cm^2, (◇) OCV, and (●) −450 mA/cm^2. (b) Results for the cell with and LSF-YSZ cathode calcined to 1373 K: (△) 450 mA/cm^2, (◇) 100 mA/cm^2, (●) OCV, (○) −100 mA/cm^2, and (□) −450 mA/cm^2.

The V-i curves for the same two cells under fuel-cell conditions, with the anodes exposed to 97% H_2-3% H_2O, are reported in Fig. 9 for operation at 1073 K, and the impedance data are given in Fig. 10. The V-i curve for the 1123 K cell is linear up to a current density of ∼1 A/cm^2, the point at which diffusion through the Ag current collector appears to limit performance. The slope of the V-i relationship and the impedance spectra (not shown) at current densities below 1 A/cm^2 indicate that the total cell ASR was 0.3 Ω cm^2. More than half of the cell losses, 0.15 Ω cm^2, were ohmic and associated with the electrolyte and the anode. The total ASR of the 1373 K cell was only slight higher, 0.4 Ω cm^2, and the ASR was
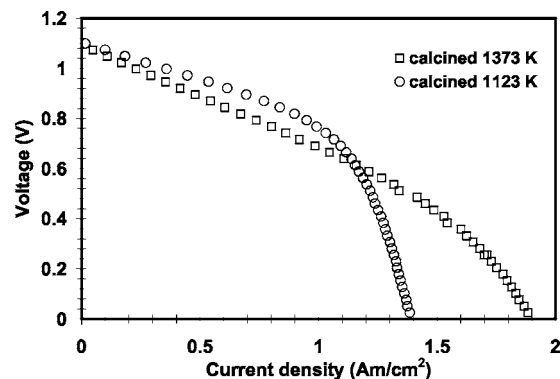
Figure 9. V-i polarization curves measured at 1073 K for two cells with LSF-YSZ electrodes. The two cells were essentially identical, except that the electrode in one was calcined to 1123 K and the other to 1373 K.
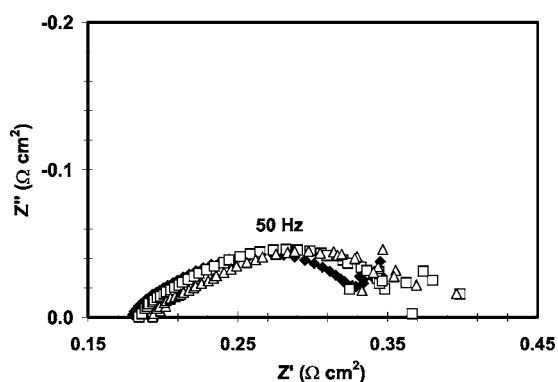
Figure 10. Cole-Cole plots for the cell calcined to 1373 K in Fig. 9, measured at OCV (◆), 300 mA/cm^2 (□), and 600 mA/cm^2 (△).

again independent of current density below 1073 K. The processes responsible for the nonlinear behavior at 973 K do not appear to be significant at 1073 K.

To help determine what changes are occurring in the LSF-YSZ electrode during lengthy operation or upon calcination to 1373 K, we examined the structure of the electrodes using SEM, with the results given in Fig. 11. Figure 11a shows the porous YSZ, prior to adding LSF. The individual YSZ crystallites exhibit terraces associated with the cubic crystal structure. Figure 11b is the micrograph for the 40 wt % LSF composite that was calcined to 1123 K. The YSZ surfaces in this sample were covered by an even layer of LSF particles that are less than 0.1 μm in size. The covering layer of LSF appears to be highly porous which would allow gas-phase molecules to easily diffuse to the YSZ surface where the three-phase boundary

(TPB) sites must be. The micrograph in Fig. 11c is that of the LSF-YSZ electrode tested for 1000 h at 973 K, followed by an additional 700 h at 1073 K. (This is the same electrode whose diffraction pattern is shown in Fig. 1b.) The aging caused sintering of the LSF particles, with the average particle size more than doubling. Finally, the composite heated to 1373 K is shown in Fig. 1d. This micrograph shows that there is further growth of the crystallites to ~0.2 μm. More significantly, the LSF does not appear to be porous, suggesting that gas-phase molecules will not be able to diffuse to the YSZ surface.

Discussion

In agreement with earlier work in our laboratory and with many other studies,[8,9,11] we have shown that LSF-based cathodes can show excellent performance as SOFC cathodes. LSF-YSZ composites prepared by impregnation and calcined at 1123 K had electrode impedances near 0.1 Ω cm^2 at 973 K even without a major effort to optimize the pore structure of the LSF. This performance level could also be achieved with relatively thick, 300 μm electrodes, implying that high-performance, cathode-supported cells can be prepared. The issue with all of the work on LSF-based electrodes using YSZ electrolytes is whether they can provide stable operation for many thousands of hours. As discussed above, the published literature leaves this question in doubt, as do the results of the present study.

To make changes that will stabilize LSF-based electrodes, it is important to understand what caused the deactivation. The fact that electrodes calcined at 1373 K showed similar characteristics to electrodes operated at 973 K for 2500 h allows some of the reasons given for deactivation in other studies to be eliminated as possibilities. For example, others have suggested that deactivation was associated with migration of the metal used for current collection within the electrode.[12] Because the current collectors on the cells calcined
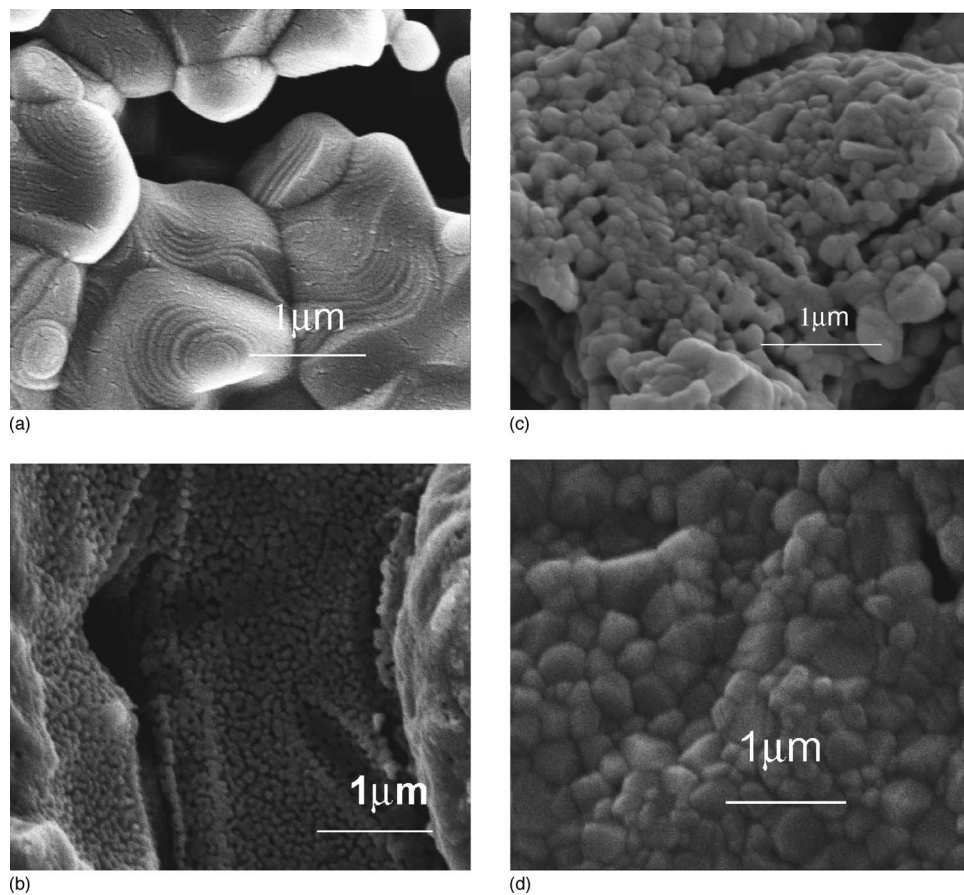
Figure 11. SEM images of (a) the porous YSZ, (b) LSF in YSZ after calcination at 1123 K, (c) LSF in YSZ after testing for 1000 h at 973 K and 700 h at 1073 K, and (d) LSF in YSZ after calcination at 1373 K.

to 1373 K were added after calcination, this cannot be the primary cause in the present study. Similarly, because the 1373 K electrode was exposed to cell operating conditions for only several hours before the measurements were made, impurities in the air feed also cannot be responsible for deactivation.

The main concern in the development of composite cathodes is whether there are solid-state reactions between the perovskite and YSZ. This is clearly the deactivation mechanism for electrodes based on $LaCoO_3$ and YSZ, because model studies have demonstrated formation of insulating phases (e.g., $La_2Zr_2O_7$) at the interface between these two oxides at temperatures as low as 973 K.[14] The elimination of solid-state reactions between LSF and YSZ was clearly the goal of earlier studies that employed ceria interlayers or additives to lower the sintering temperature of LSF.[8,9] The results of this study, however, do not suggest that solid-state reactions are responsible for the observed deactivation. Unlike $LaCoO_3$, there is no tendency to form additional phases with LSF-YSZ electrodes, even at much higher calcination temperatures. In agreement with previous work,[10] Zr doping of the perovskite phase after higher calcination temperatures was observed, but this does not appear to be the primary reason for deactivation for the following reasons. First, the shift in the LSF lattice parameter is only observed at significantly higher temperatures than those used in the preparation of the LSF-YSZ electrodes. Admittedly, this result does not completely rule out the importance of Zr doping given that XRD cannot sample the layer at the interface; but it does not provide support for this mechanism. Second, there is no significant increase in the ohmic resistance of deactivated cells, as one would expect, if deactivation of the LSF were associated with a loss in conductivity. Most importantly, electrodes made from $La_{0.8}Sr_{0.2}Fe_{0.9}Zr_{0.1}O_3$ showed performance that approached that of LSF. Taken together, these observations lead to the conclusion that solid-state reactions are not responsible for deactivation of LSF-YSZ electrodes.

The SEM data suggests that the performance changes could be associated with sintering of the LSF and the formation of a dense perovskite film over the porous YSZ. If the perovskite film prevented gaseous O_2 getting to the YSZ interface, ions formed at the LSF surface would need to diffuse through the dense film. The peak frequencies in the impedance spectra of the deactivated electrodes are low, which is indeed consistent with the rate-limiting step being an ion-diffusion process. A similar argument has been suggested as an explanation for the high impedance of LSM-YSZ electrodes prior to polarization[23] based on atomic force microscopy data which showed that LSM particles spread over a YSZ single crystal under relatively mild calcination.[23] Activation of LSM-YSZ electrodes following cathodic polarization has been suggested to be the result of openings in the LSM, due to a partial reduction of the LSM at the interface.

The formation of a dense LSF film could also provide an explanation for the strong current dependence of the impedance spectra for the deactivated LSF-YSZ electrodes. For example, higher performance of LSCo-based cathodes compared to LSM-YSZ cathodes is usually associated with the high ionic conductivity of LSCo, which extends the width of the three-phase boundary (TPB) line. Because the ionic conductivity of LSF is between that of LSM and LSCo, it is likely that the area associated with the TPB is lower that that of LSCo cathodes and will be affected by anything that changes the ionic diffusivity. If the diffusivity of oxygen ions is nonlinear, which could well occur in a mixed conductor where the diffusion coefficient has concentration and field dependences,[24] the impedance would change with current density. Furthermore, the oxygen-ion gradients across the LSF film would be similar for both anodic and cathodic polarization and the electrode impedance should be affected in a similar manner for cathodic and anodic polarization. Finally, one might expect the diffusivity of oxygen ions through the film to increase with temperature, explaining why the impedance depends more weakly on the current at higher temperature.

The classical explanation for current-dependent impedance spectra is that the charge-transfer reaction is a Butler-Volmer process.

Presumably, the charge-transfer reaction would become limiting only after sintering decreases the interfacial boundary between LSF and YSZ. For this mechanism to be operative, the activation barrier for reaction would need to be affected in the same way by negative and positive field gradients, because the electrode impedance decreases in a similar manner under both anodic and cathodic polarization. Also, the characteristic frequency of the charge-transfer reaction would need to be ~ 4 Hz, because this is the frequency of arc that is affected by an applied current. While we prefer the "diffusion" mechanism because of it is consistent with that proposed for the activation polarization of LSM-YSZ electrodes,[23] the Butler-Volmer process cannot be ruled out.

Understanding the mechanism for deactivation of LSF-YSZ electrodes is important for deciding what strategies to adopt to stabilize these materials. For example, if deactivation is due to formation of a dense LSF film, one would not expect ceria interlayers between the LSF and the YSZ to be effective in stabilizing the electrodes, independent of whether the rate-limiting step in the deactivated electrodes is oxygen diffusion or the charge-transfer reaction. In this case, the strategy for stabilizing the LSF electrodes should involve changing the morphology of the electrode structure so as to avoid forming a thick LSF film, at least in the region where the three-phase boundary exists, near the electrode-electrolyte interface. Clearly, tailoring the structure of this region has an enormous impact on the performance of LSM-YSZ electrodes.[25] We believe that similar tailoring of the electrode structure may also lead to stable LSF-YSZ cathodes.

Conclusions

The deactivation of LSF-YSZ composites is associated with a decrease in the LSF surface area and the formation of a dense LSF layer over the YSZ, rather than solid-state reactions. Strategies for stabilizing the LSF-YSZ electrodes should target ways to avoid the formation of a thick layer of LSF near the three-phase boundary.

Acknowledgments

References

1. N. Q. Minh, *J. Am. Ceram. Soc.*, **76**, 563 (1993).
2. A. Mineshige, M. Kobune, S. Fujii, Z. Ogumi, M. Inaba, T. Yao, and K. Kikuchi, *J. Solid State Chem.*, **142**, 374 (1999).
3. H. Uchida, S. Arisaka, and M. Watanabe, *Solid State Ionics*, **135**, 347 (2000).
4. T. Horita, K. Yamaji, N. Sakai, H. Yokokawa, A. Weber, and E. Ivers-Tiffee, *Electrochim. Acta*, **46**, 1837 (2001).
5. S. J. Skinner, *Int. J. Inorg. Mater.*, **3**, 113 (2001).
6. J. M. Ralph, J. T. Vaughey, and M. Krumpelt, in *Solid Oxide Fuel Cells VII*, H. Yokokawa and S. C. Singhal, Editors, PV 2001-16, p. 466. The Electrochemical Society Proceedings Series, Pennington, NJ (2001).
7. J. M. Ralph, C. Rossignol, and R. Kumar, in *Solid State Ionic Devices III*, E. D. Wachsman, K. Swides-Lyons, M. F. Carolan, F. H. Garzon, M. Liu, and J. R. Stetter, Editors, pv 2002-26, p. 133. The Electrochemical Society Proceedings Series, Pennington, NJ (2003).
8. S. P. Simner, J. F. Bonnett, N. L. Canfield, K. D. Meinhardt, V. L. Sprenkle, and J. W. Stevenson, *Electrochem. Solid-State Lett.*, **5**, A173 (2002).
9. S. P. Simner, J. F. Bonnett, N. L. Canfield, K. D. Meinhardt, J. P. Shelton, V. L. Sprenkle, and J. W. Stevenson, *J. Power Sources*, **113**, 1 (2003).
10. S. P. Simner, J. P. Shelton, M. D. Anderson, and J. W. Stevenson, *Solid State Ionics*, **161**, 11 (2003).
11. Y. Huang, J. M. Vohs, and R. J. Gorte, *J. Electrochem. Soc.*, **151**, A646 (2004).
12. S. P. Simner, M. D. Anderson, L. R. Pederson, and J. W. Stevenson, *J. Electrochem. Soc.*, **152**, A1851 (2005).
13. O. Yamamoto, Y. Takeda, and M. Noda, *Solid State Ionics*, **22**, 241 (1987).
14. M. Sase, D. Ueno, K. Yashiro, A. Kaimai, T. Kawada, and J. Mizusaki, *J. Phys. Chem. Solids*, **66**, 343 (2005).
15. J. Hole, D. Kuseer, M. Hrovat, S. Bernik, and D. Kolar, *Solid State Ionics*, **95**, 259 (1997).

16. S. P. Simner, M. D. Anderson, J. F. Bonnett, and J. W. Stevenson, *Solid State Ionics*, **175**, 79 (2004).
17. Y. Huang, K. Ahn, J. M. Vohs, and R. J. Gorte, *J. Electrochem. Soc.*, **151**, A1592 (2004).
18. W. Wang, Y. Huang, S. Jung, J. M. Vohs, and R. J. Gorte, *J. Electrochem. Soc.*, **153**, A2066 (2006).
19. M. D. Gross, J. M. Vohs, and R. J. Gorte, *Electrochem. Solid-State Lett.*, **10**, B65 (2007).
20. Y. Jiang, A. V. Virkar, and F. Zhao, *J. Electrochem. Soc.*, **148**, A1091 (2001).

21. S. McIntosh, S. B. Adler, J. M. Vohs, and R. J. Gorte, *Electrochem. Solid-State Lett.*, **7**, A111 (2004).
22. Y. Huang, J. M. Vohs, and R. J. Gorte, *J. Electrochem. Soc.*, **152**, A1347 (2005).
23. Y. Huang, J. M. Vohs, and R. J. Gorte, *Electrochem. Solid-State Lett.*, **9**, A237 (2006).
24. A. V. Virkar, *J. Power Sources*, **147**, 8 (2005).
25. J. Mertens, V. A. C. Haanappel1, C. Tropartz, W. Herzhof, and H. P. Buchkremer, *J. Fuel Cell Sci. Technol.*, **3**, 125 (2006).